

BAYESIAN OPERATIONAL MODAL ANALYSIS AND UNCERTAINTY QUANTIFICATION OF A SUPER TALL BUILDING

F.L. Zhang¹, H.B. Xiong^{2*}

¹Research Institute of Structural Engineering and Disaster Reduction, Tongji University
1239 Siping Road, Shanghai, China
e-mail: fengliangzhang@tongji.edu.cn

^{2*}Research Institute of Structural Engineering and Disaster Reduction, Tongji University
1239 Siping Road, Shanghai, China
e-mail: xionghaibei@tongji.edu.cn (corresponding author)

Keywords: Super tall building, Operational modal analysis, Bayesian, Uncertainty Quantification.

Abstract. *The dynamic characterization of structures is essential for assessing their response subjected to dynamics loads, which mainly consists of the modal properties, namely the natural frequencies, damping ratios and mode shapes. In the construction of super tall building, the modal properties will have significant change with the increase of the structure height. After the main structure is completed, the modal properties in the first few years are also attracting much attention. This paper presents the work on the operational modal analysis of a super tall building with the height of 632m situated in Shanghai, China. A recently developed fast Bayesian method is utilized to perform modal identification, which provides an effective mean to identify the modal properties and assess their accuracy. In this study, the modal properties of Shanghai Tower in different construction stages and their associated uncertainty are determined, where interesting trends are observed for the modal parameters. After the main structure is completed, a field test is also performed in a typical floor to investigate the modal properties. The results obtained would be beneficial to understand the structural behavior of this super tall building.*

1 INTRODUCTION

The Shanghai Tower, situated in Lujiazui financial and trade zone, Shanghai, China, is a super tall Mega frame-tube-outrigger structure with a height of 632m. The tower has 121 floors above the ground and 5 floors under the ground, which serve for hotels, offices, tourism, restaurant, conference room, shopping mall, etc. and can be taken as a vertical city. The internal office plane of the structure is constituted by nine rotunda superimposed on each other with eight zones divided. The curtain wall outside of the tower spins upwards, with the diameter decreasing from 83.6 m in Zone 1 to 42 m in Zone 8. As many as six two-storey out-

rigger truss and eight boxy space circular truss are set in eight electromechanical floors zone. The mega frame is composed by the boxy space circular truss and the giant column, forming a Mega frame-tube-outrigger lateral resistant system. As one of the tallest buildings in the world, the structural safety is attracting much attention. A sophisticated long-term structural health monitoring system has been designed to monitor the structural behavior in both construction and service stages. In this paper, the focus will be on the acceleration response measured in construction and after the main structure has been completed. Ambient vibration test is used to collect data with the structure under working condition. The ambient vibration tests can be divided into two parts. The first part is a series of tests in different construction stages; the second part is an ambient vibration test measuring one typical floor of the building.

2 AMBIENT VIBRATION TESTS

2.1 Test in different construction stages

To assess the structural condition under construction, fifteen ambient vibration tests are performed during about two and a half years from May, 2012 to December, 2014. The number of floors finished and the corresponding time to carry out the field test are shown in Table 1. In each test, two locations are measured. The first one is at the top of core tube while the second one is at the top composite slabs after completion of concrete pouring. In each location, 2 uniaxial accelerometers are utilized to measure the structural response. The sampling frequency is set to be 20 Hz.

Setup	1	2	3	4	5	6	7	8	9	10	11	12	13	14	15
Year/	12	12	12	12	13	13	13	13	13	13	14	14	14	14	14
Month	05	07	08	10	01	03	05	07	08	12	02	03	07	10	12
Floors	61	68	71	81	94	102	111	120	125	125	125	125	125	125	125

Table 1 Measurement time and floors

2.2 Field test in a typical floor

After the main structure is completed, it is interesting to know the modal properties of a typical floor and investigate the motion in different modes from a plan view. It is desired to measure different corners of the tube. Since the renovation has begun in the lower floors, which makes it difficult to access some corners through the tube. Meanwhile, in the measurement, higher floors are preferred since the vibration amplitude is relatively larger than those in lower floors. Taking into account above factors, 101th floor is chosen, where the filled walls inside the tube have not been finished and it is convenient to perform the sensor alignment and cable layout. Nine locations are desired to be measured bi-axially, as shown in Figure 1, including eight locations in the eight corners of the tube, and one location in the center of the whole structure. Sensor alignment is essential since it may affect the identified mode shape, and the modeling error during alignment cannot be reflected in the data analysis process. To determine the direction of the sensor channels accurately, in the beginning, a compass is used. However, this equipment cannot work well inside the building due to some unknown factors. To solve this problem, the core walls are taken as the references. Since the walls in eight corners are also different, double checking is necessary to ensure the sensors in X and Y directions are consistent.

If there were enough sensors for measuring all the 18 degrees of freedom (dofs), one could have finished the test in one setup with synchronized data. However, at the time of test only 4 channels at 2 locations can be measured at a time. It is necessary to design multiple setups to

finish the whole measurement. In order to provide common information for all the setups, two reference channels are set in location 11. During the whole measurement, the reference location is kept unchanged. The setup plan can be found in Table 2. Note that the measurement was not arranged in a particular order. This is because that at the time of measurement, some persons were still working around. Arrangement in this manner is to minimize the influence due to the noise from these construction work. Before the actual setups, a baseline test, Setup 0, was performed with all the four sensors placed near to Location 11, as shown in Figure 2 (a). This setup could provide baseline information and help detect the potential problems that may arise in some particular channels in subsequent setups.

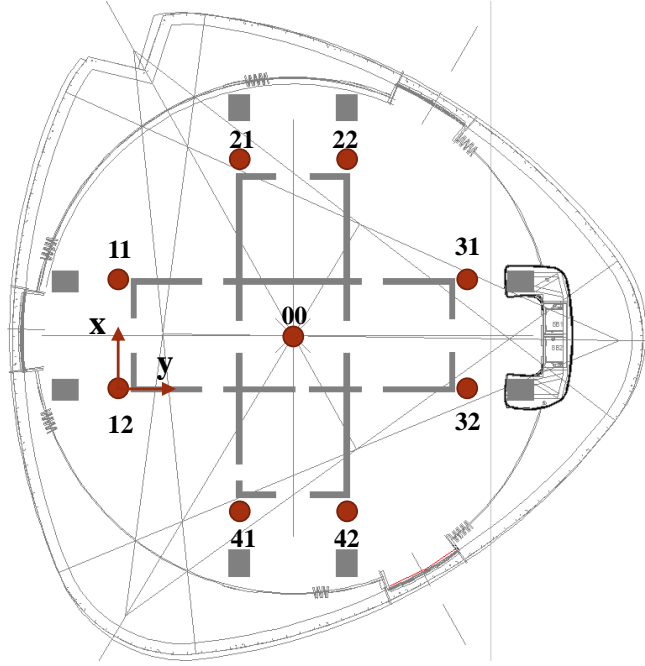


Figure 1: Setup plan

Setup	Channels 1 and 2	Channels 3 and 4
1	11	31
2	11	32
3	11	42
4	11	22
5	11	21
6	11	12
7	11	41
8	11	00

Table 2: Setup plan

In each setup, at least 40 minutes is required, including 30 minutes for data collection and 10 minutes for roving the sensor. To ensure the data quality, once the data in a particular setup is finished, some spectrum analysis will be carried out. If there is some problem, the measurement will be repeated. Figure 2 (b) shows the measurement in one particular setup. The whole measurement is performed from 10am to 7pm in a working day. The sampling frequency is set to be 2048 Hz and then in the analysis the data was decimated by 32 to a sampling rate of 64 Hz.



Figure 2: (a) All the sensor and data acquisition system; (b) Measurement in one setup

3 METHODOLOGY

To analyze the measured data, a recently developed Bayesian method is employed to perform ambient modal identification incorporating multiple setups (including single setup). The theory is outlined briefly. For the details, please refer to [1][2].

Let $\mathbf{Z}_k^{(i)} = [\text{Re } \mathcal{F}_{ik}; \text{Im } \mathcal{F}_{ik}] \in R^{2n_i}$ ($i=1, \dots, n_s$) denotes an augmented vector comprising the real and imaginary part of the FFT \mathcal{F}_{ik} of the measured data at frequency f_k in Setup i ; n_s is the number of setup; $\mathcal{D}_i = \{\mathbf{Z}_k^{(i)}\}$ denote the FFT data of the selected frequency band in Setup i and $\mathcal{D} = \{\mathcal{D}_i : i=1, \dots, n_s\}$ denote the collection of all setups. It is assumed that the data in different setups are statistically independent. Next, we define the modal parameters needed to be optimized. The modal parameter set $\boldsymbol{\theta}$ is set to be:

$$\boldsymbol{\theta} = [f_i, \zeta_i, S_i, S_{ei} : i=1, \dots, n_s; \boldsymbol{\Phi} \in R^n] \in R^{4n_s+n} \quad (1)$$

where $f_i, \zeta_i, S_i, S_{ei}$ ($i=1, \dots, n_s$) are the natural frequency, damping ratio, PSD of modal force and PSD of prediction error of Setup i , respectively; $\boldsymbol{\Phi}$ denotes the global mode shape; n is the total number of measured dofs. The global mode shape $\boldsymbol{\Phi}$ are the same in all the setups and so it can be obtained directly in the process of optimization. For the remaining modal parameters, each setup is parameterized with separate values to consider the variation of these parameters in different setups.

Assuming a uniform prior distribution, using Baye's Theorem, the posterior PDF of $\boldsymbol{\theta}$ given the data in all setups can be expressed as,

$$p(\boldsymbol{\theta} | \mathcal{D}) \propto p(\{\mathcal{D}_1, \mathcal{D}_2, \dots, \mathcal{D}_{n_s}\} | \boldsymbol{\theta}) = p(\mathcal{D}_1 | \boldsymbol{\theta}) p(\mathcal{D}_2 | \boldsymbol{\theta}) \dots p(\mathcal{D}_{n_s} | \boldsymbol{\theta}) \quad (2)$$

The modal parameters in Setup i does not depend on the modal parameters of other setups. Thus

$$p(\boldsymbol{\theta} | \mathcal{D}) \propto \prod_{i=1}^{n_s} p(\mathcal{D}_i | f_i, \zeta_i, S_i, S_{ei}, \boldsymbol{\Phi}_i) \quad (3)$$

It is more convenient to work with negative log-likelihood function (NLLF). In terms of the NLLF, this means

$$L(\boldsymbol{\theta}) = \sum_{i=1}^{n_s} L_i(\boldsymbol{\theta}_i) \quad (4)$$

where $\boldsymbol{\theta}_i = \{f_i, \zeta_i, S_i, S_{ei}, \boldsymbol{\Phi}_i\}$ with $\boldsymbol{\Phi}_i = \mathbf{L}_i \boldsymbol{\Phi} \in R^{n_i}$; $\mathbf{L}_i \in R^{n_i \times n}$ is the selection matrix; n_i is the number of measured dofs in Setup i and

$$L_i(\boldsymbol{\theta}_i) = \frac{1}{2} \sum_k [\ln \det \mathbf{C}_{ik}(\boldsymbol{\theta}_i) + \mathbf{Z}_k^{(i)T} \mathbf{C}_{ik}(\boldsymbol{\theta}_i)^{-1} \mathbf{Z}_k^{(i)}] \quad (5)$$

where $\det(\cdot)$ denotes the determinant ;

$$\mathbf{C}_{ik}(\boldsymbol{\theta}_i) = \frac{S_i D_{ik}}{2} \begin{bmatrix} \boldsymbol{\varphi}_i \boldsymbol{\varphi}_i^T & 0 \\ 0 & \boldsymbol{\varphi}_i \boldsymbol{\varphi}_i^T \end{bmatrix} + \frac{S_{ei}}{2} \mathbf{I}_{2n_i} \quad (6)$$

denotes the theoretical covariance matrix of the FFT data at the k -th frequency abscissa in Setup i ; $\mathbf{I}_{2n_i} \in R^{2n_i}$ denotes the identity matrix;

$$D_{ik}(f_i, \zeta_i) = [(\beta_{ik}^2 - 1)^2 + (2\zeta_i \beta_{ik})^2]^{-1} \quad (7)$$

with $\beta_{ik} = f_i / f_k$.

Theoretically, maximizing posterior PDF in (3) is equivalent to minimizing the NLLF in (4) to obtain the MPV of modal parameters. However, if directly performing the optimization, there will be some computational problems, i.e., the optimization process is ill-conditioned and if the number of modal parameters is too large, it may be not converged. In view of this, well-separated mode case is focused. The NLLF is reformulated as follows by eigenvalue decomposition technique, and it allows efficient computation.

$$\begin{aligned} L(\boldsymbol{\theta}) = & -(\ln 2) \sum_{i=1}^{n_s} n_i N_{fi} + \sum_{i=1}^{n_s} (n_i - 1) N_{fi} \ln S_{ei} \\ & + \sum_{i=1}^{n_s} \sum_k \ln(S_i D_{ik} \|\mathbf{L}_i \boldsymbol{\varphi}\|^2 + S_{ei}) + \sum_{i=1}^{n_s} S_{ei}^{-1} d_i - \boldsymbol{\varphi}^T \mathbf{A}(\boldsymbol{\varphi}) \boldsymbol{\varphi} \end{aligned} \quad (8)$$

where N_{fi} denotes the number of FFT ordinates in the selected frequency band in Setup i ; and

$$\mathbf{A}(\boldsymbol{\varphi}) = \sum_{i=1}^{n_s} S_{ei}^{-1} \sum_k (\|\mathbf{L}_i \boldsymbol{\varphi}\|^2 + S_{ei} / S_i D_{ik})^{-1} \mathbf{L}_i^T \mathbf{D}_{ik} \mathbf{L}_i \in R^{n \times n} \quad (9)$$

$$\mathbf{D}_{ik} = \text{Re } \mathcal{F}_{ik} \text{Re } \mathcal{F}_{ik}^T + \text{Im } \mathcal{F}_{ik} \text{Im } \mathcal{F}_{ik}^T \in R^{n_i \times n_i} \quad (10)$$

$$d_i = \sum_k (\text{Re } \mathcal{F}_{ik}^T \text{Re } \mathcal{F}_{ik} + \text{Im } \mathcal{F}_{ik}^T \text{Im } \mathcal{F}_{ik}) \quad (11)$$

Based on (8), partial analytical solutions of the MPV of modal parameters have been derived, leading to a fast iterative algorithm that can be practically implemented even for a large number of dofs and setups. For details, please refer to [1].

In addition to the MPV, Bayesian method can also be used to determine the associated posterior covariance matrix, which is equal to the inverse of the Hessian matrix. Analytical expressions for calculating the Hessian matrix have been derived and for the details, please refer to [2]. This makes the posterior uncertainty of modal parameters can be determined analytically without resorting to finite difference.

4 DATA ANALYSIS

4.1 Data in different construction stages

In this study, the data in the second location with the length of 20 min were analyzed. Figure 3 shows the PSD spectrum of the measured data at the first time of the measurement. Clear peaks can be found indicating structural modes. It is seen that the natural frequency of the first mode is larger than 0.3 Hz.

Figure 4 shows the identified natural frequencies and damping ratios in different construction stages for the first two modes, where each parameter is shown with a dot at the MPV and an error bar covering ± 2 posterior standard deviations. It is seen that the natural frequencies tend to decrease following with the increase of the number of floors finished. After the main structure was completed, the increase speed becomes slow and tends to be stable. It is

also found that the uncertainty of the natural frequency is quite small, which also verify that the decrease of the natural frequency is not attributed to the identified error since there is no overlap of the error bar among neighbored setups. For the damping ratio, whose values are all around or less than 1%, with the increase of floors, no obvious trend can be found. Comparing with the natural frequency, damping ratios have a relatively high uncertainty.

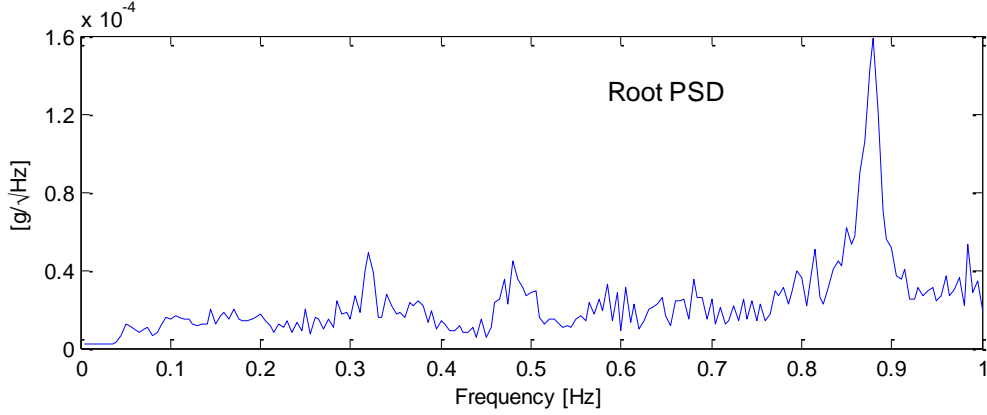


Figure 3: PSD spectrum in the first measurement

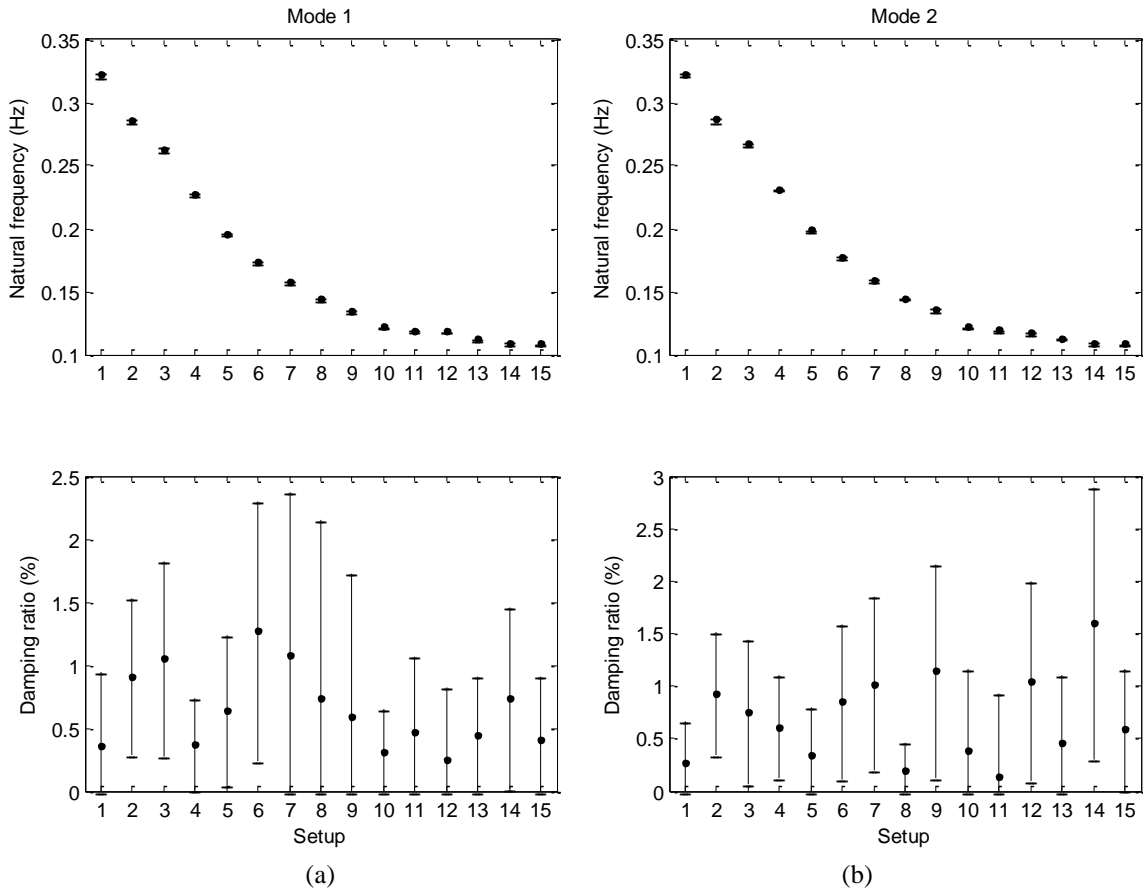


Figure 4: Identified modal parameters in different construction stages: (a) Mode 1, (b) Mode 2

4.2 Data in a typical floor

Based on the field test, nine setups data were collected. Figure 5 shows the PSD spectrum of Setup 1. It is seen that below 1 Hz, there are about eight obvious peaks. Based on the

Bayesian method mentioned, Modal identification will be performed on these eight potential modes.

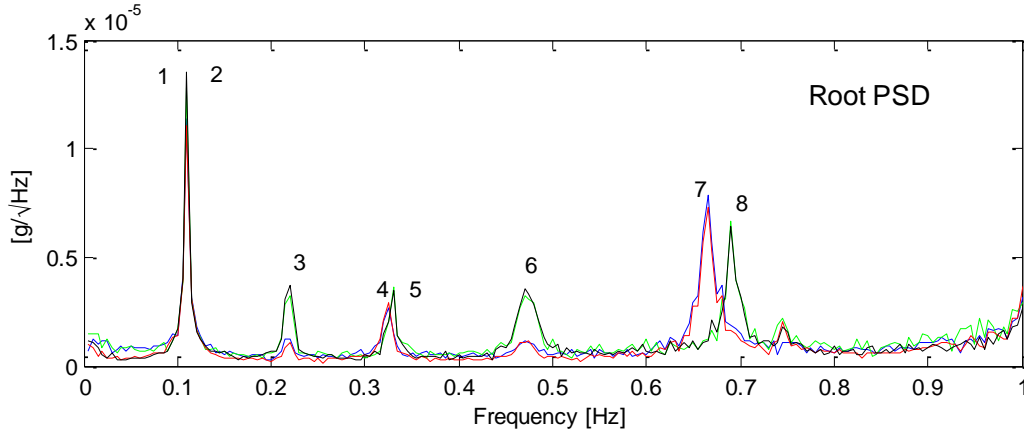


Figure 5: PSD spectrum of the data in Setup 1

Note that the first two modes are closely-spaced modes. According to the analysis before, these two modes are mainly along x and y directions, respectively. The Bayesian method incorporating multiple setups introduced in last section now can only work well on the well separated modes. Therefore, the data in x and y directions are analyzed separately. For other modes, i.e., Mode 3 to Mode 8, since from the singular value decomposition (SVD) spectrum, all the modes are well-separated modes and so they are identified using the data in both x and y directions together. Figure 6 to Figure 9 show the identified natural frequencies, damping ratios and PSD of modal force in different setups of Modes 1 to 8, where each parameter is shown with a dot at the MPV and an error bar covering ± 2 posterior standard deviations. It is seen that the natural frequencies have a small variations among different setups with a small posterior uncertainty, while this is not the fact for the damping ratio and PSD of modal force, especially for the PSD of modal force, which can reflect the environment changing across several hours. It is also interesting to find that the posterior uncertainty of modal parameters can reflect the data quality consistently and the uncertainty of these three modal parameters are larger than those of other setups, for example, setup 4 of mode 1, setup 2 of mode 2, setup 3 of mode 3, setup 4 of mode 4, setup 4 of mode 5, setup 4 of mode 7 and setups 7 and 8 of mode 8.

Figure 10 to Figure 13 show the mode shapes of the eight identified modes. The values above the figures are averaged natural frequency and damping ratio of nine setups with the values in the parenthesis being the posterior c.o.v. (coefficient of variations). Consistent with the investigation above, the posterior c.o.v. of natural frequency is less than 1%, which is much smaller than those of damping ratio with the order of magnitude of a few tens percent. It is seen that the first two modes are translational modes in x and y directions, respectively. The third mode is the first torsional mode of the building with the torsion center located at the center of the tube. Similar to the mode 1 to mode 3, the fourth to sixth modes are translational modes in x and y directions, and the second torsional mode, respectively. The mode 7 and mode 8 are also translational modes in x and y directions. From the mode shapes, it is seen that although the design of this structure is special, the mode shapes are regular. Table 3 shows the comparison between averaged posterior c.o.v. and the sample c.o.v. among different setups. It is seen that the latter tend to be larger than the former, but they have similar order of magnitude, although these two quantities reflect the different concepts.

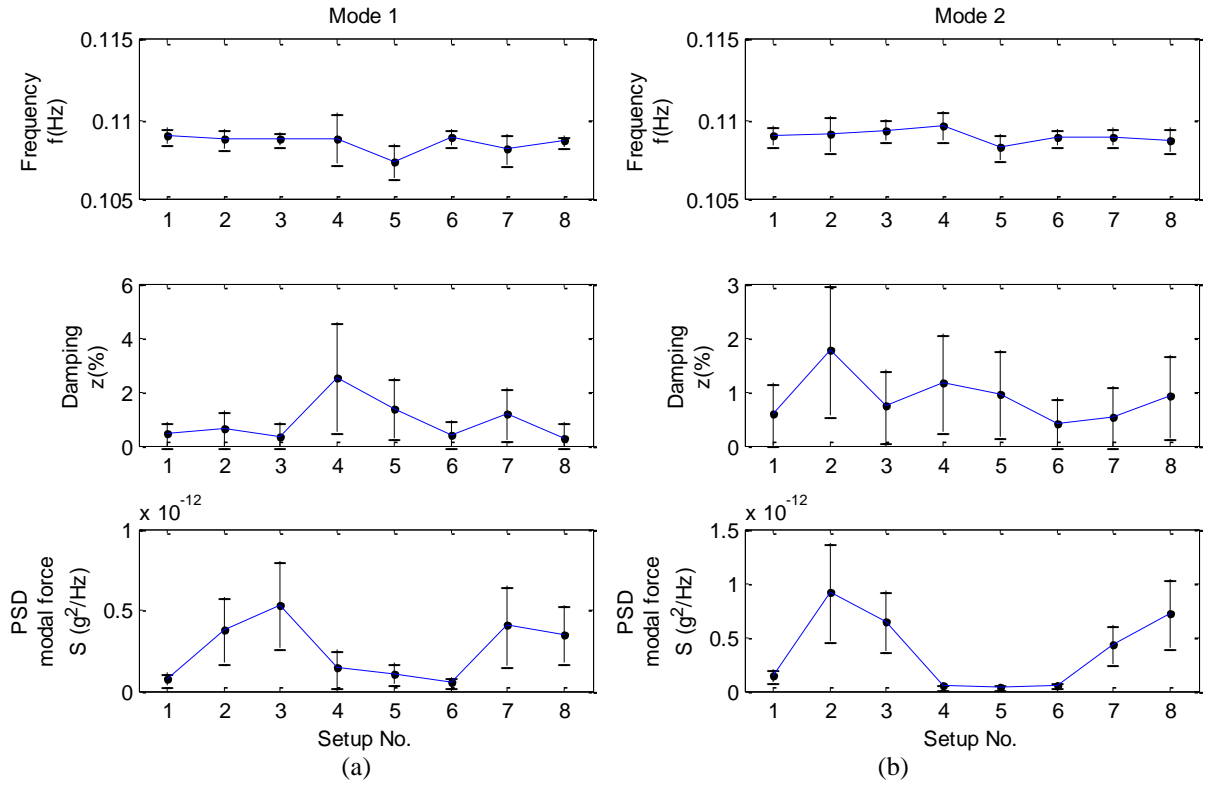


Figure 6: Identified modal parameters and the associated uncertainty: (a) Mode 1; (b) Mode 2

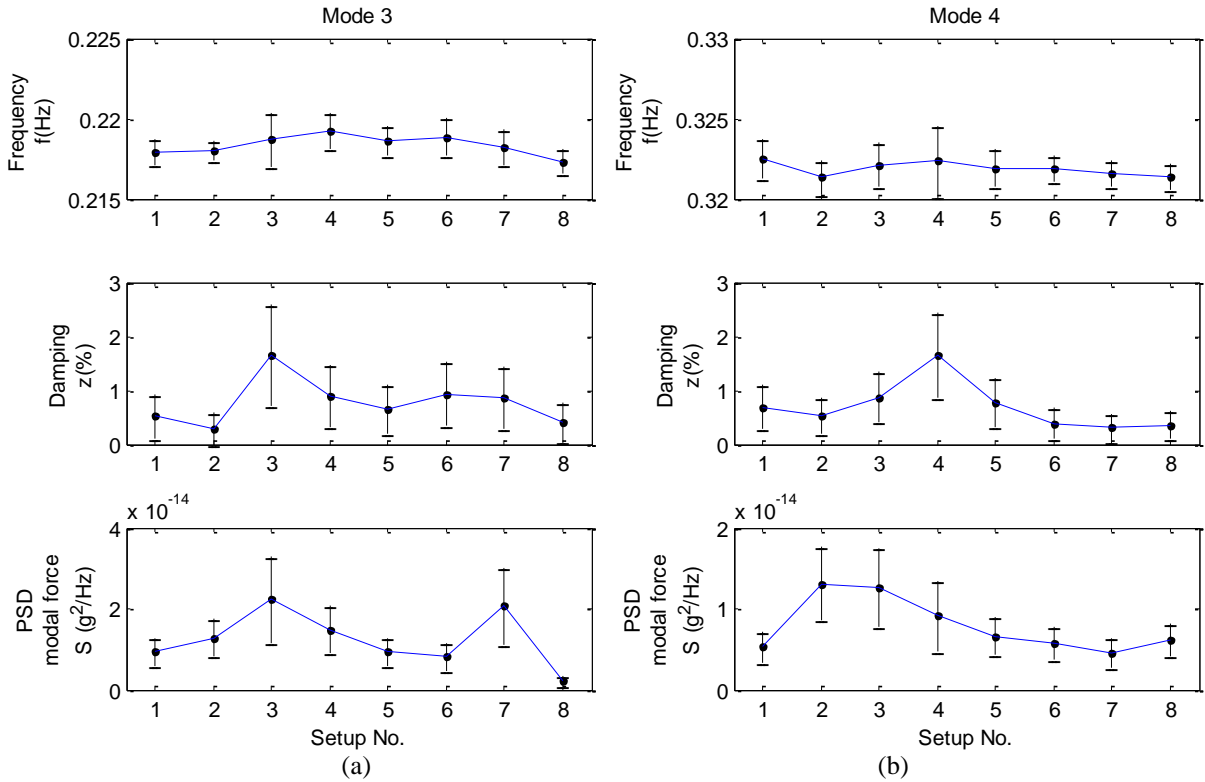


Figure 7: Identified modal parameters and the associated uncertainty: (a) Mode 3; (b) Mode 4

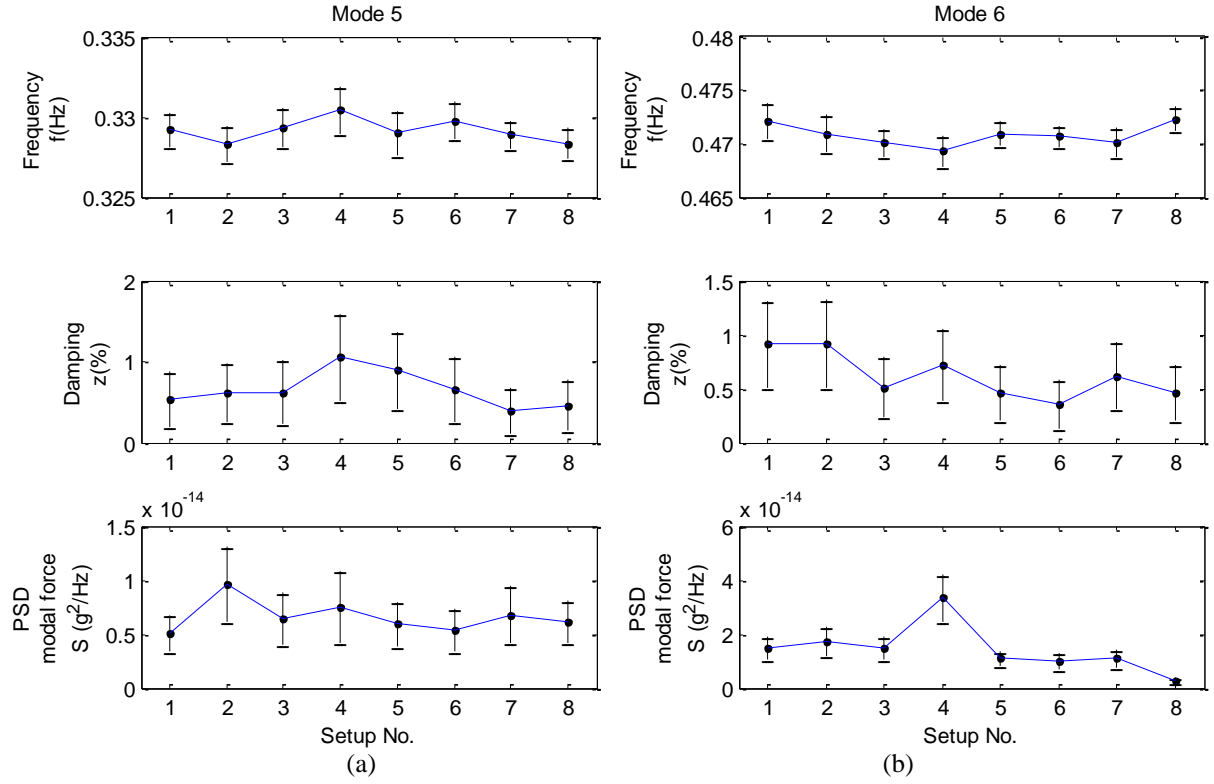


Figure 8: Identified modal parameters and the associated uncertainty: (a) Mode 5; (b) Mode 6

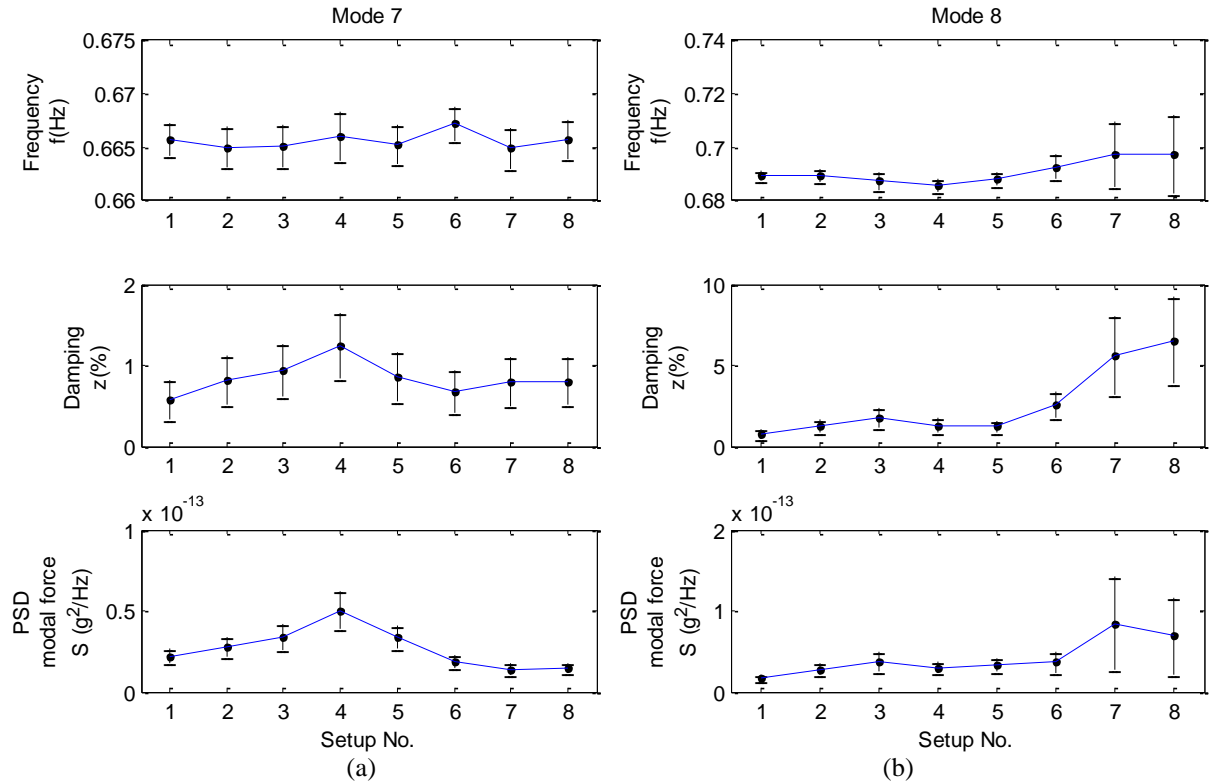
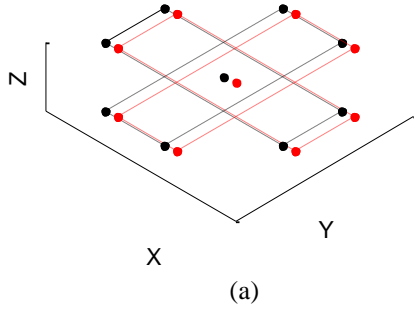


Figure 9: Identified modal parameters and the associated uncertainty: (a) Mode 7; (b) Mode 8

0.1086Hz(0.35%), 0.892%(61%)



0.1090Hz(0.34%), 0.885%(45%)

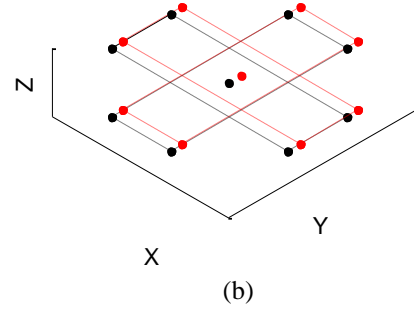
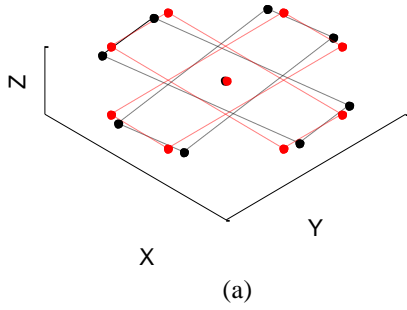


Figure 10: Identified mode shapes: (a) Mode 1; (b) Mode 2

0.218Hz(0.24%), 0.78%(37%)



0.322Hz(0.19%), 0.70%(32%)

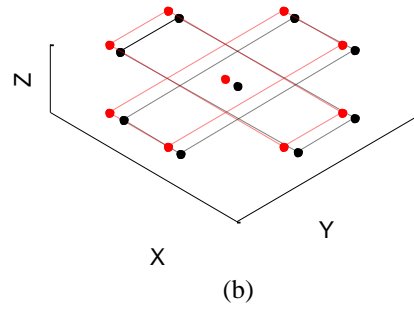
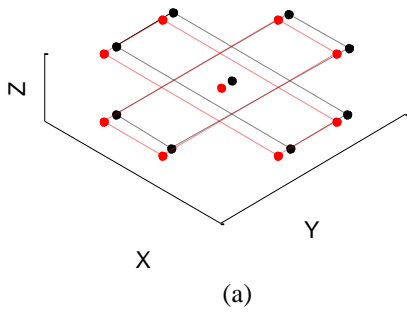


Figure 11: Identified mode shapes: (a) Mode 3; (b) Mode 4

0.329Hz(0.18%), 0.66%(31%)



0.471Hz(0.14%), 0.62%(26%)

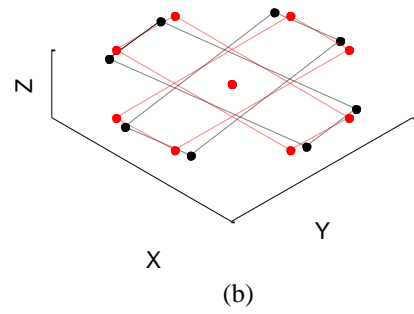
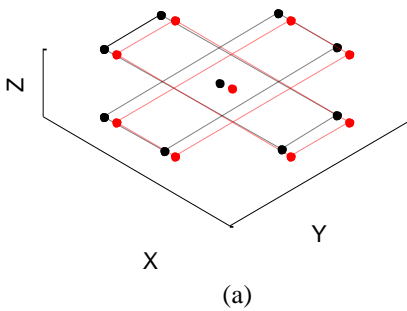


Figure 12: Identified mode shapes: (a) Mode 5; (b) Mode 6

0.666Hz(0.14%), 0.84%(19%)



0.691Hz(0.40%), 2.64%(18%)

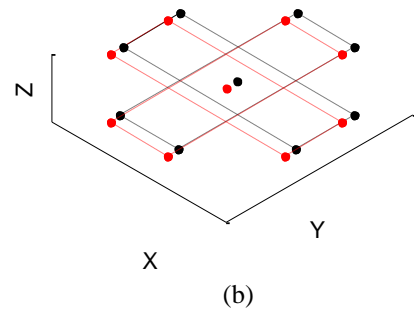


Figure 13: Identified mode shapes: (a) Mode 7; (b) Mode 8

	Mode	1	2	3	4	5	6	7	8
f(%)	PC.O.V.	0.35	0.34	0.24	0.19	0.18	0.14	0.14	0.40
	SC.O.V.	0.50	0.37	0.28	0.14	0.21	0.22	0.11	0.64
z(%)	PC.O.V.	61	45	37	32	31	26	19	18
	SC.O.V.	87	49	54	63	33	34	24	83

Table 3 Posterior c.o.v. and sample c.o.v.

5 CONCLUSIONS

This paper presents the work on ambient vibration tests and modal identification using a Bayesian method. To monitoring the modal properties in different construction stages, 15 field tests have been carried out with the number of the floors increasing from 61/F to 125/F. In this process, the natural frequencies decrease obviously at first, and then tend to be stable after the main structure is completed. The posterior uncertainty of natural frequency is quite small, indicating the identification of this quantity is accurate. This also reflects that the decrease of natural frequency is not attributed the identification error since there is no overlap for the error bar. For the damping ratio, which have a larger uncertainty, no obvious trend can be found in different construction stages. The ambient vibration test in a typical floor is also presented to investigate the modal properties in this floor by nine setups due to the limitation of the number of sensors. It is found that there are more than 8 modes below 1 Hz, including three translational modes in x direction, three translational modes in y direction and two torsional modes. The identified results show that although the design of this structure is highly innovative and full of art, the dynamic characteristics are regular. By investigating the posterior uncertainty of modal parameters in different setups, the problematic data in some setup can be reflected, where all the modal properties in this setup will have a larger uncertainty. Finally, by comparing the posterior c.o.v. and sample c.o.v. among different setups, it is found although these two quantities are with different concepts but they have similar order of magnitude.

6 ACKNOWLEDGEMENTS

This paper is funded by the National Basic Research Program of China (973 Program) (Project No. 2014CB049100) and the Grant from the Fundamental Research Funds for the Central Universities, China (Grant No. 2014KJ040). The financial support is gratefully acknowledged. The authors would like to thank Prof. Weixing Shi, professor at Tongji University, for providing logistic support for the field tests, Mr. Xiang Ou, graduate student at Tongji University, for participating the field tests.

7 REFERENCES

- [1] S.K. Au and F.L. Zhang, Fast Bayesian ambient modal identification incorporating multiple setups. *Journal of Engineering Mechanics, ASCE*, **138**(7), 800-815, 2012.
- [2] F.L. Zhang, S.K. Au and H.F. Lam, Assessing uncertainty in operational modal analysis incorporating multiple setups using a Bayesian approach, *Structural Control and Health Monitoring*, **22**(3), 395-416.